Energy demand and yield enhancement for roof mounted photovoltaic snow mitigation systems

Iver Frimannslund [a,*], Thomas Thiis [a], Louise V. Skjøndal [a], Thomas Marke [b]

[a] Norwegian University of Life Sciences, Department of Building- and Environmental Technology, NO-1432 Ås, Norway
[b] University of Innsbruck, Institute of Geography, 6020 Innsbruck, Austria

ARTICLE INFO

ABSTRACT

The deployment of photovoltaic (PV) systems in the built environment is limited by lacking structural capacity of existing roofs. PV snow mitigation systems can overcome such limitations by reducing heavy snow loads through active snow melting. The competitiveness of such systems is influenced by how much energy is needed to melt the snow and how much the yield is increased by reducing the snow cover on the modules. This study aims to quantify the energy consumption and yield enhancement of PV snow mitigation systems using numerical simulations. With an adapted energy balance snow model simulating Snow Water Equivalent (SWE), the energy consumption from melting snow as well as the snow cover duration on the modules are estimated. The snow cover duration is then used as input in PV yield simulations to quantify the yield enhancement. Different types of snow load climates are investigated. The results show that the energy consumption is < 11.8 kWh/m^2 and the yield enhancement < 3 kWh/m^2 per year depending on the climate and the melting limit. Climates with low characteristic snow loads give the lowest energy consumption and the highest yield enhancement. For the investigated climate with the lowest snow load (50-year return period snow load = 0.7 kN/m^2) the enhancement is larger than the consumption giving a positive energy balance of 0.6 kWh/m^2. The relative influence on the energy production is + 1 % to −13 % of the production of PV systems without active snow mitigation.

© 2022 The Author(s). Published by Elsevier B.V. This is an open access article under the CC BY license (http://creativecommons.org/licenses/by/4.0/).

1. Introduction

Photovoltaic (PV) systems are increasing in popularity and are expected to do so in the future as well [31]. In the built environment, roof surfaces are attractive for the installation of PV systems due to often being unused, accessible for maintenance, and in proximity to the consumer. However, not all roofs are suitable for the installation of PV systems as the irradiance conditions can be suboptimal [27] and the building roof may lack structural capacity.

One of the reasons some existing buildings lack structural capacity is due to being built at a time where the environmental loads used in the design of structures were lower than modern standards require. The characteristic snow load used in the design of buildings is commonly determined with the return period concept defining the load with a set probability of being exceeded. Modern design standards such as the Eurocode standard, ASCE and ISO use characteristic snow load with 50-year return period (YRP), equaling a 2 % yearly probability of being exceeded. How-ever, previous building codes have used lower return period loads in the design. Prior to the use of international standards, these loads were commonly determined on a national basis and large variations exist depending on the year the structural design was made. To summarize some return periods used for snow load in national building codes Croce et al. [7] elaborate that a 30 YRP was used in the Canadian Building Code until 2005, while 25 YRP is currently used in Russia and 100 YRP in Japan. In Norway, a 5 YRP snow load was used before 1999 [20]. If the current character-istic snow load is higher than what was used in the design of the building, building owners are often prevented from installing PV systems. The structural capacity of building roofs is not commonly considered in studies concerning the rooftop potential for PV sys-tems [19], but is a known limitation for PV deployment in the built environment [25]. Thus, existing estimates of rooftop PV potential may be significantly overestimated.

To increase PV deployment on existing building roofs which lack structural capacity, PV systems that melt snow by applying heat to the modules surface have been developed [9]. Such systems are often referred to as *PV snow mitigation systems* or *self-heating PV systems*. PV snow mitigation systems which reduce snow loads are designed with a low angle tilt to retain the snow on the modules

---

* Corresponding author.
  E-mail address: iver.frimannslund@nmbu.no (I. Frimannslund).

during melting. Such systems have been used in Norway since the 2016 and are increasing in popularity. The typical configuration of a PV snow mitigation system is shown in Fig. 1.

There are also PV snow mitigation systems that intend only to increase the yield by having higher tilts and sliding snow off the module surface [32] as yield losses from snow is a challenge for PV systems in cold climates [14]. PV snow mitigation systems which are designed for reducing snow loads monitor the snow load on the roof and trigger a heat flux when the load exceeds a defined threshold. Commonly only the peak loads are reduced and all the snow on the modules is not removed. However, reducing the peak loads potentially contribute to increased yield as the snow cover duration on the modules is shortened.

The profitability of PV snow mitigation systems compared to ordinary PV systems is influenced by how much energy is used to reduce the snow load as well as how much energy is gained from reducing the snow cover. Actively mitigating snow is likely to reduce the profitability compared to ordinary PV systems, but the advantage is that a higher share of the surfaces in the urban environment can be utilized for PV power production. Using energy to mitigate the snow loads can thus be considered a trade-off to utilize the unused surfaces which without active snow mitigation would be indisposable for PV production. No previous studies have quantified the long-term influence of active snow mitigation with PV systems.

2. Method

In this study, we combine an energy balance snow model with PV yield simulations to quantify the energy consumption and power production of PV snow mitigation systems. The outline of the method is given in Fig. 2. The energy balance snow model simulates the buildup of snow represented by the Snow Water Equivalent (SWE) using hourly meteorological data. The model is adapted so that SWE exceeding a threshold limit is subjected to a heat flux from the PV system. From this model, the energy required to melt the snow and the duration of snow cover on the modules is calculated. PV yield simulations are used to determine the yield of PV systems with a configuration typical for the PV snow mitigation system. To quantify how the yield is enhanced by snow mitigation systems, the duration of the snow cover from the energy balance snow model is used as input to the PV yield simulation.

As both the power production and energy consumption of the system is dependent on climate, the simulation method is applied

Fig. 1. A PV snow mitigation system installed on a warehouse in Oslo. The system is designed by Innos [12].
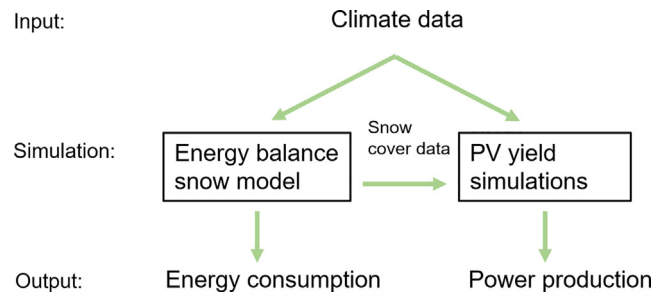

Fig. 2. Outline of the method used in the study.

to four locations with different climatic conditions. The locations are chosen based on having different characteristic snow loads and irradiance conditions. An overview of the climate data for the chosen locations are shown in Table 1.

Tromsø is located high north and has a low Global Horizontal Irradiance (GHI) and a high snow load. Oslo is at a lower latitude and has a higher GHI than Tromsø and a lower characteristic snow load. Munich has relatively high irradiance and a low snow load, while Davos has high irradiance and a high snow load. The varying climatic conditions contribute to a better understanding of the system's energy production and demand for different locations. The following sections present the modelling approach in detail.

2.1. Energy balance snow model

2.1.1. The ESCIMO model

The energy balance snow model used in this study is a physically based point snow surface model called the Energy Snow Cover Balance Integrated Model (ESCIMO v.2) by Marke et al. [18]. Based on hourly climatic data, the energy and mass balance of the snowpack is calculated to yield the Snow Water Equivalent (SWE) (the amount of liquid water contained within the snowpack in mm). Hourly data from six climatic variables is required, including ambient temperature (K), relative humidity (%), wind speed (m/s), precipitation (mm/h), global horizontal irradiance (W/m2), and incoming longwave radiation (W/m2). The energy balance equations calculate the following heat fluxes for a single-layer snowpack: sensible heat, latent heat, advective heat, as well as the short- and longwave radiation balance. The model has recently been evaluated in different climatic and environmental settings with other energy balance snow models by Krinner et al. [15] and has relatively high accuracy. The hourly temporal resolution of the model is superior to many other existing snow models, but the snowpack is represented by a single layer in the model, meaning that the properties of the snowpack are considered to be homogeneous. This simplification influences the layered properties of the snow which influences heat transfer in the snowpack [22] and sublimation fluxes [28]. Moreover, the model is describing the relevant processes at the point-scale, hence spatial differences in snow cover conditions are not accounted for by the model. Given the limited size and as a result rather homogeneous conditions on flat roofs, this model characteristic is assumed to have little effects on the results of this study.

As input to the model, the ERA5 reanalysis dataset is used [10]. The database provides consistent climate data from 1979 to present in an hourly temporal resolution. Data from 1980 to 2021, equaling 41 complete winters is used as input to adequately capture the climatic variability at the study locations. The spatial resolution of the data is 0.25x0.25° corresponding to below 28x28 km depending on the latitude. As the grid often extends beyond the borders of the investigated location of interest (the city) and have a mean elevation often higher than this point of interest, the sim-

Table 1
Irradiance and snow load data for the four investigated locations. GHI is the Global Horizontal Irradiance obtained from Meteonorm [21]. S_{50} is the simulated characteristic 50-year return period snow load obtained according to the method described in 2.1.1.

Location	Tromsø	Oslo	Munich	Davos
Latitude	69.6° N	59.9° N	48.4° N	48.8° N
GHI (annual average) [kWh/m^2]	735	972	1198	1432
S_{50} [kN/m^2]	5.9	3.0	0.7	7.9

ulated SWE will not always accurately depict the local snow load climate of the cities, which can change significantly with local topography [6].

2.1.2. Model adaption for PV snow mitigation

In this study, the model is adapted to incorporate the heat flux transferred from the PV modules replacing a constant soil heat flux assumed to be 2 W/m2 in the standard model setup for natural settings. As mentioned in the introduction, the PV snow mitigation systems function by monitoring the snow load on the roof and applying heat to the modules when the snow load exceeds a threshold limit. The SWE the model estimates is analogous with the snow load in N/m^2. A condition is imposed that a melting heat flux from the PV panel is added to the snowpack when the snow load exceeds the threshold limit. The energy transferred to the snowpack is then calculated as the sum of hours with applied power as defined by Eq. (1).

$$E_{cons} = \frac{\sum_i^T P_{PV}}{Y} \tag{1}$$

Where P_{PV} is the power per PV module area in W/m^2, T is the number of hours with applied power during the simulation, Y is the number of years in the simulation and E_{cons} is the total energy consumed per module area in Wh/m^2/year during the simulation. In this study, P_{PV} is set to 300 W/m^2 which is similar to what is used in existing PV snow mitigation systems. The model does not consider the erosion of snow from the roof [17] or passive heat loss from the building roof [33] at the present time.

2.1.3. PV snow mitigation model validation

To investigate the accuracy of the adapted energy balance snow model, a real snow melting event from a building with a PV snow mitigation system is simulated and compared with measured snow load data. The event occurred on a flat roof building in Porsgrunn, Norway. The building lacks structural capacity due to being designed for a lower snow load than given by current regulations. The building owners previously relied on manual snow removal after heavy snow fall, but decided to install a PV snow mitigation system in 2019. The PV system has an installed capacity of 1137 kWp and constitutes of 3670 modules. After installation, the maximum snow load limit was set to 80 kg/m^2. The roof snow load is monitored by 12 load cells connected to the PV mounting rack.

The investigated event is from a heavy snow fall that occurred on the 10th and 11th of March where the snow load increased from an average of 0 to 62.0 kg/m^2 with single sensors measuring as high as 77.6 kg/m^2. As the snow load was nearing the melting threshold and was still increasing, the operators decided to initiate melting at approximately 08:00 the morning of March 11th. Unfortunately, there is limited information on the timeline for applying power after 08:00 and if power was applied to the whole system at once or only parts.

To simulate the event, measured data from nearby weather stations is used as input in the energy snow balance model. The longwave radiation is estimated using a cloud-based radiation model for all sky conditions [16]. As the measured temperature on the PV modules is approximately 2 °C lower than the temperature from the nearest weather station, the input temperature is applied

a correction of −2°C. Melting is initiated at 08:00 with an applied power of 300 W/m^2 for the remainder of the simulation. The simulated and measured snow load is shown in Fig. 3.

The simulated buildup of snow shows a good agreement with the measured snow load but builds up slightly slower and ends up 21.5 % lower than the average peak load. When power is applied to the modules, the reduction of the snow load is delayed by approximately 2 h both in the measurements and simulations. This likely occurs as energy is required to increase the temperature of the snowpack to 0 °C (reducing the snowpack's cold content) before the energy induces melting of the snowpack and as it takes time for the water to drain. During melting, the snow load is reduced slightly slower than the measured load for an applied effect of 300 W/m^2. During the measurements, the snow load reduction ceases close to midnight on March 11th when the snow load is reduced to an acceptable level. On the morning of the 12th, melting is continued and most of the snow is melted. The simulations consistently apply power and do not capture these variations.

The comparison between measured and simulated snow load in the event indicates that both the buildup and melting of the snowpack are reproducible with the simulation method. However, the comparison is not sufficient to determine the energy efficiency of the system as data lacks for the timeline of applied power in the measurements.

2.1.4. Snow load melting thresholds

To generalize the method and make it applicable to different climates without case-specific knowledge of the structural capacity, the melting threshold defining when the PV heat flux is triggered is set using the return period concept as described in the introduction. To determine the return period snow loads, energy balance snow model simulations without any PV heat flux are performed for the four investigated locations. A distribution is fitted to the annual maximum snow loads of the dataset using the Akaike Information Criterion [2]. The return period loads are then obtained as the value with the desired probability of being exceeded. The distribution fit to the data for the four cities is shown in Fig. 4 and the return period loads are shown in Table 2.

Fig. 4 shows that the simulated snow loads exhibit different characteristics for the different climates. For Munich, heavy snow loads occur infrequently and are best approximated by the lognormal distribution. In Tromsø and Oslo, the occurrence of heavy snow loads is more frequent and follows the gamma distribution best. In Davos, heavy snow loads occur frequently, best approximated with a Weibull distribution. The shape of the distributions influences the return periods snow loads given in Table 2. Distributions with longer tails (such as for Munich) contribute to a larger relative difference in the melting threshold compared to short tail distributions (such as for Davos).

As the PV system utilizes load capacity on the roof, the melting limit (S_{lim}) is the return period snow load subtracted by the self-weight of the PV system as defined in Eq. (2):

$$S_{lim} = S_{returnperiod} - g_{PV} \tag{2}$$

Where $S_{return\ period}$ is the return period load from Table 2 and g_{PV} is the self-weight of the PV system. PV systems commonly weigh between 0.1 and 0.5 kN/m^2, depending on mounting and roof bal-
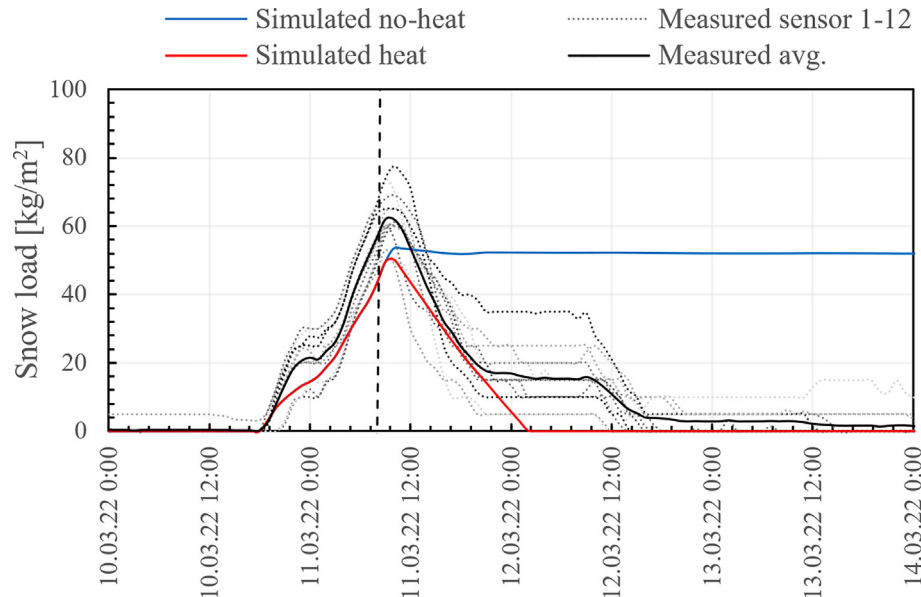
Fig. 3. Measured and simulated snow load during a snow fall event in Porsgrunn, Norway. The vertical dashed line signifies when power was applied to the modules.
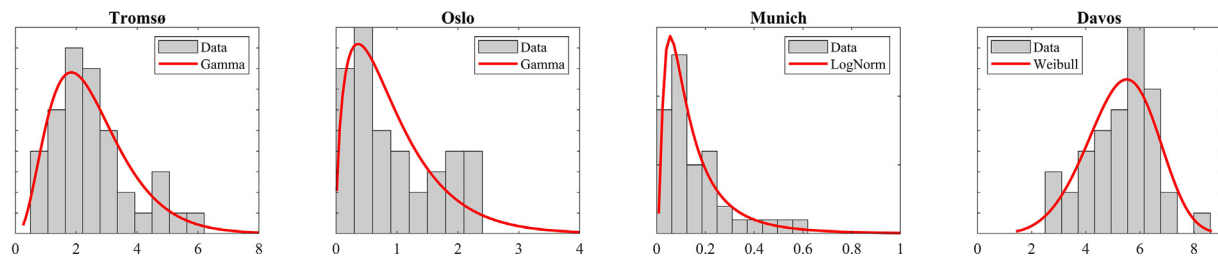

Fig. 4. Histogram of maximum annual snow load in kN/m^2 with the best fitting distribution for the four investigated locations.

Table 2
Snow loads for a 50-, 30-, 20-, 10- and 5-year return period for the investigated locations in kN/m^2 as well as the Coefficient of Variation (COV) of the annual maximum loads.

Location	Tromsø	Oslo	Munich	Davos
Snow load distribution	Gamma	Gamma	Lognormal	Weibull
Return period snow loads				
S_{50}	5.9	3.0	0.7	7.9
S_{30}	5.4	2.7	0.6	7.5
S_{20}	5.0	2.4	0.5	7.3
S_{10}	4.3	1.9	0.4	6.9
S_5	3.5	1.4	0.2	6.4
$CoV_{annual\ max}$	0.54	0.77	0.85	0.24

last. Here g_{PV} is set to 0.2 kN/m^2, representing a system without heavy ballast. An example of how the melting limit influence the SWE for a single winter in Tromsø, Norway is shown in Fig. 5.

The snow cover duration is calculated as the number of hours with a snow cover larger than 2 mm SWE. This limit is chosen as light can be transmitted for snow covers thinner than this, causing the module to produce power and passively shed snow [23].

2.2. PV yield simulations

To quantify the yield of PV snow mitigation systems, energy yield simulations are performed in PVsyst 7.2 [24]. The system configuration and electrical design is set to be representative of typical PV snow mitigation systems with an east and west facing orientation with a module tilt of 10° as shown in Fig. 1. A 100 kW string inverter is used with 21 strings and 19 modules per string

on average. This yields a ratio between the nominal PV capacity and inverter power of approximately 1.25. The modules are the LR6-60PE 310 M from Longi Solar and the inverter is the PVS-100-TL from FIMER. For climate and irradiance data, Meteonorm 8.0 is used. Meteonorm generates site specific data from ground stations and satellite data to generate hourly climate data. PV yield simulations are generally accurate with the largest uncertainty being the input irradiance [30].

To account for the loss in power production due to snow covered modules (in this study referred to as *snow loss*), we use the snow cover duration from the energy balance snow model as input to PVsyst. The average monthly snow cover duration is calculated from the 41 years of simulated SWE and defined as monthly snow loss in PVsyst. Commonly, snow is cleared earlier from solar panels than a roof surface due to the module being tilted and having a low friction surface [34]. However, PV snow mitigation systems are
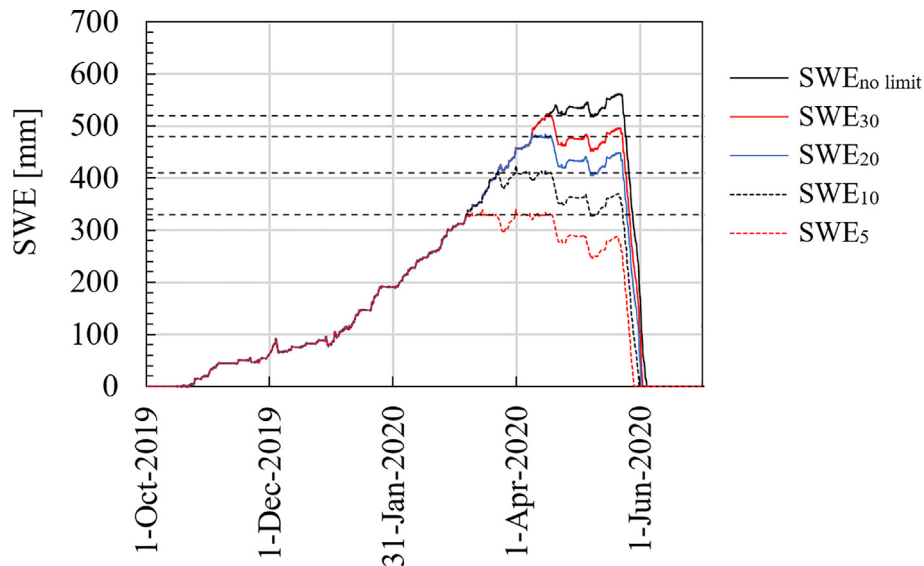
Fig. 5. Single year simulation of SWE for different return period melting limits (subscript in legend) in Tromsø the winter of 2019–2020. The horizontal dashed lines signify the SWE threshold for when power is applied.

designed to retain the snow on the module surface and an assumption can be made that the snow duration on the modules is equal to the roof.

3. Results

The result section is divided into three sections. In section 3.1 the energy demand required to maintain the snow load below the threshold limit is presented, section 3.2 shows how the reduction of snow cover influences the power production and section 3.3 shows the net energy balance of PV snow mitigation systems.

3.1. Energy consumption

The yearly average energy consumption (E_{cons} as defined in Eq. (1)) is shown in Fig. 6a while Fig. 6b shows the average annual snow load reduction amount (ΔS_{avg}). The energy amount used per kilo of mitigated snow is shown in Table 3.

The amount of snow melted by the PV system (ΔS_{avg}) in Fig. 6b shows an exponential increase with decreasing return period melting limits. Tromsø and Oslo exhibit an almost identical development in snow load reduction amount with a magnitude maximum ΔS_{avg} = 26.4 kg/m^2 and 18.3 kg/m^2 respectively. Munich and Davos have similar reduction amount (the maximum being ΔS_{avg} = 11.7 kg/m^2) and have a similar development with return period melting limits although they are characterized by very different snow load climates. This can be explained by ΔS_{avg} being dictated by the magnitude of the snow load as well as the shape of the distribution of the snow load. Higher magnitude snow loads contribute to more snow being removed from the roof and as well does the length of the distribution tail as longer tails result in a larger difference between the maximum snow loads and the melting limits. Although Davos has the highest snow loads, the short tail distributions reduce the snow load reduction amounts, contrary to Munich which has the lowest snow load with a long-tailed distribution. The result of this is that if normalizing the snow load
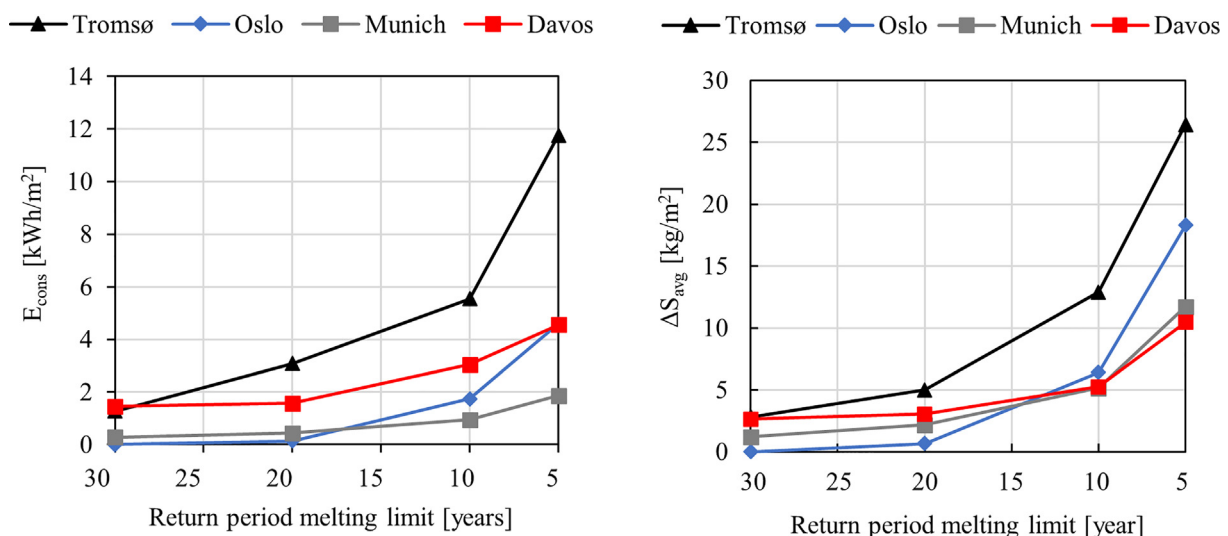

Fig. 6. a) Average annual energy consumption (E_{cons}) and b) average annual snow load reduction amount (ΔS_{avg}) per year for a PV snow mitigation system with different return period melting limits.

Table 3

Average melting energy per kilogram of snow (E_{avg}) for the different locations.

Location	Tromsø	Oslo	Munich	Davos
E_{avg} [kWh/kg]	0.48	0.24	0.19	0.52

reduction amount to the 50-year snow load, the longer tail distributions and high CoV's (such as Oslo and Munich) have a higher average snow load reduction amount than distributions with shorter tails with low CoV's (Such as Davos).

The melting energy per kilo of snow (E_{avg}) in Table 3 varies with climate. In general, higher snow load climates give a higher E_{avg}. This is influenced by snowfall and snow load reduction is more frequent in high snow load climates. The thermal mass of the snow results in more energy required to heat up the snow to reduce the snowpack's cold content before the energy is used to melt the snowpack as experienced in the validation case. Higher snow load climates commonly also have lower average temperatures which contribute to a larger amount of cold content in the snowpack. A high E_{avg} indicates a low efficiency of the active melting process. Variations in the climate-related efficiency contribute significantly to variations in the total energy consumption.

The average annual energy consumption (E_{cons}) in Fig. 6a is influenced by the snow load reduction amounts (as given in Fig. 6b) and the efficiency of the system (Table 3). Tromsø has the highest snow load reduction amounts and a low melting efficiency giving the highest consumption (E_{cons} = 11.8 kWh/m^2). Davos has relatively stable snow load reduction amounts for the varying melting limits compared to the other climates but has the lowest efficiency. This results in stable and high energy consumption for all the melting limits in Davos (E_{cons} < 4.56 kWh/m^2). In Oslo, the snow load reduction amount increases strongly with melting limit and has the second highest consumption for the 5-year return period melting limit (E_{cons} = 4.59 kWh/m^2) although the efficiency is the second highest. Due to a poor distribution fit for high snow loads no melting occurs in Oslo for the 30-year return period melting. Munich has the lowest consumption for return period melting limits smaller than 20 years (E_{cons} < 1.87 kWh/m^2), due to having a small snow load reduction amount and high efficiency.

3.2. Influence of snow mitigation on power production

The energy yield of a PV system with a configuration as described in section 2.2 is simulated with snow losses obtained from the simulated snow cover duration from the energy balance snow model. The power production of a PV system without active melting is shown in Table 4, while Fig. 7 shows the monthly snow loss.

Fig. 7 shows that the monthly snow loss varies significantly between the locations. Snow rich climates such as Tromsø and Davos have monthly snow losses of more than 80 % for 5 months or more during the year. Oslo has more intermediate snow losses and is only above 50 % for 3 months of the year. The snow losses in Munich are significantly smaller being less than 22 % in the most snow rich month. The red bar shows the difference in snow losses between the 5-year return period melting limit and no melting limit. For Oslo, Tromsø, and Davos only small reductions in monthly snow losses occur in the spring months of April and May. Munich, however, which has a very low melting limit 5-year return period melting limit, experiences a more significant reduction in snow losses during all the winter months.

Table 4 shows that the production of the PV system (E_{prod}) shows an increase with decreasing latitude except for Davos. In high latitude climates, the irradiance is lower, and the snow losses are more significant. Davos has an abnormally low yield for its latitude and arises from the heavy snow losses for the largest parts of the year. The yield enhancement from the reduced snow cover duration is shown in Fig. 8.

Here we see that the yield enhancement ($E_{enhance}$) is small for Oslo, Tromsø and Davos which show only minor difference in the monthly snow losses from snow melting ($E_{enhance}$ < 1 kWh/m^2). The yield enhancement in Munich is low for the return period melting limit between 30 and 10 years but increase significantly for the 5-year return period melting limit ($E_{enhance}$ = 3 kWh/m^2).

Table 4

PV system power production for the four investigated locations. The yield is given by two measures which have a linear relationship. Specific yield (kWh/kWp/year) is commonly used in the PV discipline while E_{prod} (kWh/m^2/year) is in line with the units used in the rest of the study. The system design is described in section 2.2.

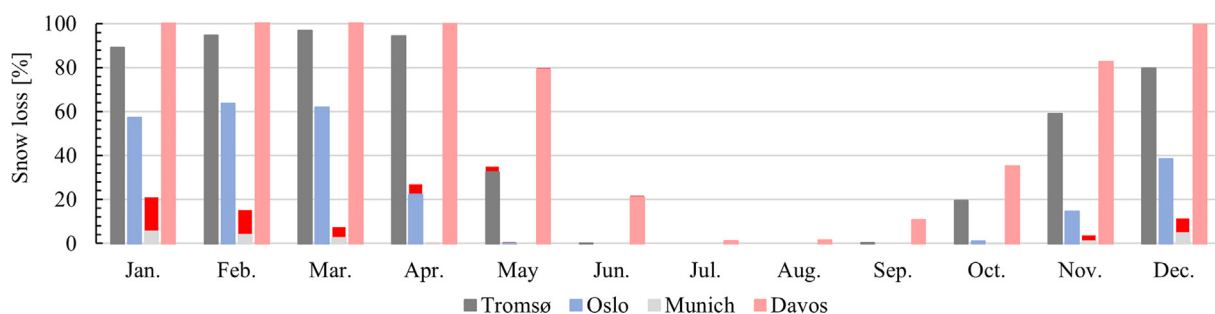| Location	Tromsø	Oslo	Munich	Davos
E_{prod} [kWh/m^2/year]	86	141	190	113
Specific yield [kWh/kWp/year]	456	751	1011	600

Fig. 7. Monthly snow loss [%] obtained from the energy balance snow model. The difference in snow loss between the 5-year return period melting limit and no melting limit is illustrated by the red bars. (For interpretation of the references to colour in this figure legend, the reader is referred to the web version of this article.)
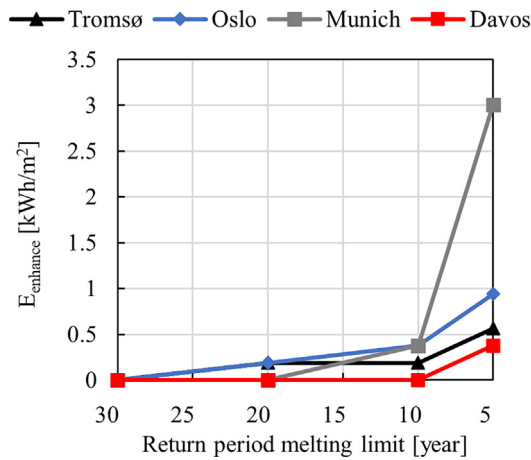
Fig. 8. The yield enhancement ($E_{enhance}$) per year from the decrease in snow losses for different return period melting limits in relation to a PV system without snow mitigation (given in Table 3).
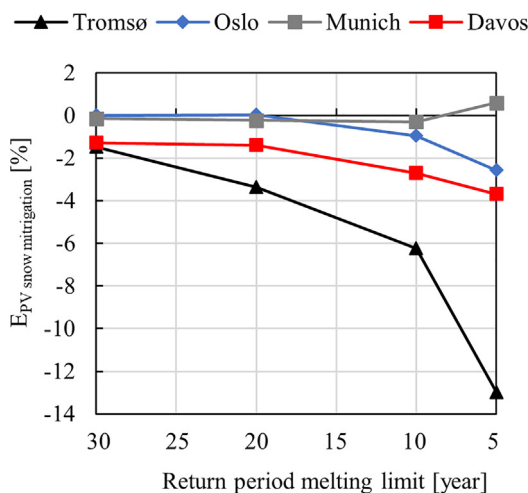

Fig. 9. Simulated influence of actively mitigating snow ($E_{PV\ snow\ mitigation}$) for varying return period melting limits for the four locations.

This occurs as the 5-year return period melting limit in Munich is so low that almost all snow is melted from the roof.

3.3. Net energy balance

The net influence of consumption and yield enhancement from snow melting ($E_{PV\ snow\ mitigation}$) is calculated according to Eq. (3) and is shown in Fig. 9.

$$E_{PVsnowmitigation} = \frac{E_{enhance} - E_{cons}}{E_{prod}} \qquad (3)$$

The simulated influence of actively mitigating snow ($E_{PV\ snow\ mitigation}$) in Fig. 9 is negative for most return period melting limits as the consumption exceeds the yield enhancement. The energy balance is lowest for the high snow load climates of Tromsø ($E_{PV\ snow\ mitigation}$ < -13 %) and Davos ($E_{PV\ snow\ mitigation}$ < -3.7 %) having a high energy consumption and little yield enhancement. Oslo has no energy consumption or yield enhancement for the 30-year return period melting limit due to a poor distribution fit for the high snow load data, and has a negative influence for the 20-, −10 and 5-year return period melting limits ($E_{PV\ snow\ mitigation}$ < -2.6 %). The energy balance in Munich is little influenced by the

PV snow mitigation function for the return period melting limits of 30-, 20- and 10-years, but is positive for the 5-year return period melting limit ($E_{PV\ snow\ mitigation}$ < +0.6 %) as the enhancement exceeds the consumption.

4. Discussion

The results from this study show that the mechanisms which contribute to the net energy balance of PV snow mitigation systems strongly depends on the climate the PV system is situated in. For snow rich climates, the energy consumption dominates the energy balance as the yield enhancement is close to insignificant. The long-lasting winter results in that although the peak load is reduced, a significant amount of snow is still on the modules, and the influence on yield is small. Any increase in yield occurs in the spring months when the snow cover duration is shortened as less snow is necessary to be passively melted in order for the module to be cleared. However, the shortening of the snow cover duration is only in the magnitude of days and has a small total impact on the yield. The single year simulation in Fig. 5 illustrates this clearly. For climates with little snow, reducing the peak load during mid-winter can significantly enhance the yield as significant snow melting can occur any month of the year, and the module surface can entirely be cleared. In this study, the system is operated to only reduce peak snow loads to ensure that the total load on the roof does not exceed the roof capacity but using the system with the intent of keeping a clear module surface may provide a larger positive energy balance. Nonetheless, the results indicate that the PV snow mitigation systems are more suitable for low snow load climates as less energy is needed to melt the snowpack and the yield can be enhanced significantly due to earlier snow clearance.

The results also indicate the suitability of PV snow mitigation systems to structures with different structural capacity here represented by the melting limit. In climates with significant snow loads, structures which are not severely lacking capacity is more suitable for PV snow mitigation systems as the melting limit strongly influences the consumption but not the yield enhancement. In low snow load climates, the differences in consumption with melting limit are smaller, and larger yield gains can be obtained for low-melting limits, resulting in melting limit having low influence on the energy balance.

To indicate the validity of the results, the simulated average energy amount per kilo of snow is compared to experimental values from previous studies of PV snow mitigation. A study from Anadol [3] on the melting performance of PV modules with resistive wires presents the energy amounts required to melt snow. This study presents data from several melting episodes where the energy amount used to melt the snow as well as the snow depth is given, but not the density of the snow. If it is assumed that the density of the snow (which is specified to be freshly fallen) has a typical value of 100 kg/m^3 [26], an energy amount of 0.18–0.4 kWh/kg is calculated for snow load reduction between 4 and 9 cm and a module tilt of 10°. Aarseth et al. [1] used payback time calculations with data from field measurements to study the energy economy of PV snow mitigation systems using the forward-bias method for modules with a tilt of 10°. In their study, an energy consumption of 0.05–0.15 kWh/kg is obtained through measurements, but no details of snow depth or density are given. In the present study, the simulated average energy amount is between 0.19 and 0.52 kWh/m^2 depending on the climate (Table 3). The simulated energy amount is thus similar to the values from Anadol [3] and higher than given by Aarseth et al. [1]. Energy efficiency during melting is dependent on a number of factors including snow and air temperature, snow thickness, wind speed which

can explain the range in values in both measurements and in the simulations. In order to increase the validity of the results presented here, more experimental data of the melting efficiency should be provided. In addition to the uncertainty in system efficiency, other uncertainties in the modelling approach include:

- neglecting snow erosion and roof heat loss in the energy balance snow model,
- coarse spatial resolution for the ERA5 data,
- inaccuracies in the unadapted energy balance snow model,
- suboptimal temporal resolution of snow losses in PVsyst (only monthly values).

The first three listed uncertainties have implications for the accuracy of the estimation of the SWE on the building roof for the specific locations. Neglecting snow erosion and heat loss in the energy balance snow model will contribute to an overestimation of the SWE. The impact of this simplification can be indicated by the *shape coefficients* used in snow load design standards for buildings which are used to convert ground snow loads to roof snow loads. For flat roofs, a shape coefficient of 0.8 is used in the international, the European and the American design standards [4,5,13], although this is suggested by field measurements to be a conservative estimate [29]. Thus, the simulated SWE may overestimate the snow load by more than 20 %, which can be expected to have a similar impact on the energy consumption.

Coarse spatial resolution in climate models generally leads to underestimation of climate extremes [11]. However, as the average elevation of the grid cell is higher than the average location of the investigated cities, it can be argued that the coarse spatial resolution of ERA contributes to an overestimation of SWE in this study. For example, in Davos, the average elevation of the grid cell in ERA5 is 1999 m.a.s.l. when Davos actually resides at 1560 m.a.s.l. Moreover, incoming shortwave radiation in the ERA5 data might differ from actual values at Davos due to effects of orographic shadowing that are not adequately represented due to the coarse representation of topography in ERA5. Thus, the results likely overestimate the SWE for the location of the city, but may still underestimate the SWE for the area of the grid cell on average. Inaccurate simulated snow load can create biases in the energy consumption and the monthly snow losses used in the energy yield simulations. Future studies should account for the above-mentioned uncertainties to increase the accuracy of the simulating net energy balance of PV snow mitigation systems.

As research on rooftop snow mitigation systems progress, more complicated strategies for system operation than applying power when the snow load reaches the threshold limit will develop. Ideally, the strategy should take into account climatic conditions during melting as well as weather forecast to increase the chances of successfully reducing the load, minimizing the energy consumption and to achieve the desired level of structural safety [8]. Such strategies can involve melting during favourable conditions (i.e., in ambient temperatures above freezing) to create load buffers. This should be considered in future work on the energy consumption of PV snow mitigation systems.

5. Conclusions

Actively mitigating snow with PV systems is a measure to increase PV deployment on existing roof surfaces which are indisposable for ordinary PV systems due to lacking structural capacity. The profitability of PV systems which mitigate snow is impacted by the energy used to mitigate snow, as well as how a reduced snow cover on the modules improves the yield. In this study, an adapted energy balance snow model and energy yield simulations are applied to quantify the energy consumption and yield enhance-

ment of PV snow mitigation systems in different climatic conditions and environmental settings. To indicate the validity of the simulation method, the adapted energy balance snow model is used to reproduce a melting event with a PV snow mitigation system, showing good agreement with measured snow load data in the buildup and melting of the snow load. Simulated results with long time series of meteorological data show that in climates with significant snow loads the energy demand is high as significant amounts of snow are melted and snow losses are marginally reduced in spring, giving low yield enhancement. In climates with low snow loads, the energy demand is lower, and for low melting limits the yield enhancement is more significant. The relative influence on the energy production depends on the production of the PV system in the specific climate and is between + 1 % to −13 % of the production of a system without active snow mitigation. The simulated energy efficiency of the active snow mitigation is compared with experimental values and exhibits a reasonable agreement, but more data on the system performance is required to increase the validity of the findings. Future work on simulating energy consumption of PV snow mitigation with energy balance snow models should be improved to better represent the accumulated SWE on building roofs and to consider more advanced operation of the snow mitigation system.

Data availability

Data will be made available on request.

Declaration of Competing Interest

The authors declare that they have no known competing financial interests or personal relationships that could have appeared to influence the work reported in this paper.

References

[1] Aarseth, B. B., Øgaard, M. B., Zhu, J., Strömberg, T., Tsanakas, J. A., Selj, J. H. & Marstein, E. S. (2018, 26 September 2018). Mitigating Snow on Rooftop PV Systems for Higher Energy Yield and Safer Roofs. *EU PVSEC 2018: 35th European Photovoltaic Solar Energy Conference and Exhibition*, Brusells.

[2] Akaike, H. (2011). Akaike's Information Criterion. In Lovric, M. (ed.) *International Encyclopedia of Statistical Science*, pp. 25-25. Berlin, Heidelberg: Springer Berlin Heidelberg.

[3] M.A. Anadol, Snow melting on photovoltaic module surface heated with transparent resistive wires embedded in polyvinyl butyral interlayer, Solar Energy 212 (2020) 101–112, https://doi.org/10.1016/j.solener.2020.10.073.

[4] ASCE. (2013). *Minimum Design Loads for Buildings and Other Structures*.

[5] CEN. (2003). Eurocode 1, actions on structures—Part 1-3: General actions—Snow loads. Brussels, Belgium.

[6] P. Croce, P. Formichi, F. Landi, P. Mercogliano, E. Bucchignani, A. Dosio, S. Dimova, The snow load in Europe and the climate change, Clim. Risk Manage. 20 (2018) 138–154, https://doi.org/10.1016/j.crm.2018.03.001.

[7] P. Croce, P. Formichi, F. Landi, F. Marsili, Harmonized European ground snow load map: Analysis and comparison of national provisions, Cold Regions Sci. Technol. 168 (2019), https://doi.org/10.1016/j.coldregions.2019.102875.

[8] D. Diamantidis, M. Sykora, D. Lenzi, Optimising monitoring: standards, reliability basis and application to assessment of roof snow load risks, Struct. Eng. Int. 28 (3) (2018) 269–279, https://doi.org/10.1080/10168664.2018.1462131.

[9] I. Frimannslund, T. Thiis, A feasibility study of photovoltaic snow mitigation systems for flat roofs, Tech. Trans. 81–96 (2019), https://doi.org/10.4467/2353737XCT.19.073.10724.

[10] Hersbach, H., Bell, B., Berrisford, P., Biavati, G., Horányi, A., Muñoz Sabater, J., Nicolas, J., Peubey, C., Radu, R., Rozum, I., Schepers, D., Simmons, A., Soci, C., Dee, D., Thépaut, J-N. (2018). *ERA5 hourly data on single levels from 1979 to present*. Copernicus Climate Change Service (C3S) Climate Data Store (CDS) (ed.).

[11] C.E. Iles, R. Vautard, J. Strachan, S. Joussaume, B.R. Eggen, C.D. Hewitt, The benefits of increasing resolution in global and regional climate simulations for European climate extremes, Geosci. Model Dev. 13 (11) (2020) 5583–5607, https://doi.org/10.5194/gmd-13-5583-2020.

[12] Innos. (2022). *Innos AS*. Available at: www.innos.no (accessed: 18.01.2022).

[13] ISO, ISO 4355 Bases for design of structures, Determination of snow loads on roofs, ISO, 2013, p. 42.

[14] B.P. Jelle, The challenge of removing snow downfall on photovoltaic solar cell roofs in order to maximize solar energy efficiency—Research opportunities for the future, Energy Build. 67 (2013) 334–351, https://doi.org/10.1016/j.enbuild.2013.08.010.

[15] G. Krinner, C. Derksen, R. Essery, M. Flanner, S. Hagemann, M. Clark, A. Hall, H. Rott, C. Brutel-Vuilmet, H. Kim, et al., ESM-SnowMIP: Assessing snow models and quantifying snow-related climate feedbacks, Geosci. Model Dev. 11 (2018) 5027–5049, https://doi.org/10.5194/gmd-11-5027-2018.

[16] G.E. Liston, K. Elder, A meteorological distribution system for high-resolution terrestrial modeling (MicroMet), J. Hydrometeorol. 7 (2) (2006) 217–234, https://doi.org/10.1175/JHM486.1.

[17] Z. Liu, Z. Yu, F. Zhu, X. Chen, Y. Zhou, An investigation of snow drifting on flat roofs: Wind tunnel tests and numerical simulations, Cold Regions Sci. Technol. 162 (2019) 74–87, https://doi.org/10.1016/j.coldregions.2019.03.016.

[18] T. Marke, E. Mair, K. Förster, F. Hanzer, J. Garvelmann, S. Pohl, M. Warscher, U. Strasser, ESCIMO.spread (v2): Parameterization of a spreadsheet-based energy balance snow model for inside-canopy conditions, Geosci. Model Dev. 9 (2016) 633–646, https://doi.org/10.5194/gmd-9-633-2016.

[19] Melius, J., Margolis, R. & Ong, S. (2013). *Estimating Rooftop Suitability for PV: A Review of Methods, Patents, and Validation Techniques*. United States: Medium: ED; Size: 35 p. 10.2172/1117057.

[20] V. Meløysund, K.R. Lisø, J. Siem, K. Apeland, Increased snow loads and wind actions on existing buildings: reliability of the norwegian building stock, J. Struct. Eng. 132 (11) (2006) 1813–1820, https://doi.org/10.1061/(ASCE)0733-9445(2006)132:11(1813).

[21] Meteonorm. (2020). *Features - Data sources*. Available at: https://meteonorm.com/en/meteonorm-features (accessed: 18.10.21).

[22] Nuijten, A., Høyland, K. V., Kasbergen, C. & Scarpas, T. (2016). Modelling the thermal conductivity of melting snow layers on heated pavements. *8th International Conference on Snow Engineering*: 263-269.

[23] R.E. Pawluk, M. Rezvanpour, Y. Chen, Y. She, A sensitivity analysis on effective parameters for sliding/melting prediction of snow cover on solar photovoltaic panels, Cold Regions Sci. Technol. 185 (2021), https://doi.org/10.1016/j.coldregions.2021.103262.

[24] PVsyst SA. (2021). PVsyst 7.2. route du Bois-de-Bay 107, Satigny, Switzerland.

[25] E.H. Richards, K. Schindel, T. Bosiljevac, S.F. Dwyer, W. Lindau, A. Harper, Structural considerations for solar installers : an approach for small, simplified solar installations or retrofits, United States (2011), https://doi.org/10.2172/1034886.

[26] M.B. Rohrer, L.N. Braun, H. Lang, Long-term records of snow cover water equivalent in the swiss Alps: 1. Analysis, Hydrol. Res. 25 (1–2) (1994) 53–64, https://doi.org/10.2166/nh.1994.0019.

[27] D.J. Sailor, J. Anand, R.R. King, Photovoltaics in the built environment: A critical review, Energy Build. 253 (2021), https://doi.org/10.1016/j.enbuild.2021.111479.

[28] G.A. Sexstone, D.W. Clow, D.I. Stannard, S.R. Fassnacht, Comparison of methods for quantifying surface sublimation over seasonally snow-covered terrain, Hydrol. Process. 30 (19) (2016) 3373–3389, https://doi.org/10.1002/hyp.10864.

[29] T.K. Thiis, M. O'Rourke, Model for snow loading on gable roofs, J. Struct. Eng. 141 (12) (2015) 04015051, https://doi.org/10.1061/(ASCE)ST.1943-541X.0001286.

[30] Urraca, R. H., Thomas; Lindfors, V. Anders; Riihelä, Aku; Martinez-de-Pison, Javier, Francisco; Sanz-Garcia, Andres. (2018). Quantifying the amplified bias of PV system simulations due to uncertainties in solar radiation estimates. *Solar Energy*, 176: 663-677.

[31] VDMA. (2020). *International Technology Roadmap for Photovoltaic, Results 2019*.

[32] C. Yan, M. Qu, Y. Chen, M. Feng, Snow removal method for self-heating of photovoltaic panels and its feasibility study, Solar Energy 206 (2020) 374–380, https://doi.org/10.1016/j.solener.2020.04.064.

[33] M. Zhao, J. Srebric, R.D. Berghage, K.A. Dressler, Accumulated snow layer influence on the heat transfer process through green roof assemblies, Build. Environ. 87 (2015) 82–91, https://doi.org/10.1016/j.buildenv.2014.12.018.

[34] M.B. Øgaard, B.L. Aarseth, Å.F. Skomedal, H.N. Riise, S. Sartori, J.H. Selj, Identifying snow in photovoltaic monitoring data for improved snow loss modeling and snow detection, Solar Energy 223 (2021) 238–247, https://doi.org/10.1016/j.solener.2021.05.023.